ORIGINAL RESEARCH

Recovery of Dysregulated Genes in Cancer-Related Lower Limb Lymphedema After Supermicrosurgical Lymphaticovenous Anastomosis – A Prospective Longitudinal Cohort Study

Johnson Chia-Shen Yang [1,2], Lien-Hung Huang[1,2], Shao-Chun Wu [3,4], Yi-Chan Wu[1,4], Chia-Jung Wu[1,4], Chia-Wei Lin[1,4], Pei-Yu Tsai[1,4], Peng-Chen Chien[1,4], Ching-Hua Hsieh[1,2]

[1]Division of Plastic and Reconstructive Surgery, Department of Surgery, Kaohsiung Chang Gung Memorial Hospital, Kaohsiung, Taiwan; [2]Graduate Institute of Clinical Medical Sciences, College of Medicine, Chang Gung University, Taoyuan, Taiwan; [3]Department of Anesthesiology, Kaohsiung Chang Gung Memorial Hospital, Kaohsiung, Taiwan; [4]Chang Gung University College of Medicine, Taoyuan, Taiwan

Correspondence: Ching-Hua Hsieh, Graduate Institute of Clinical Medical Sciences, Chang Gung University College of Medicine, 123 Dapi Road, Niaosong District, Kaohsiung City, 833, Taiwan, Tel +886-7-7317123, ext.8002, Fax +886-7-7354309, Email prs581126@gmail.com

Purpose: This study aims at profiling the expression of dysregulated genes in circulating monocytes of patients with cancer-related lower limb lymphedema before and after treatment with supermicrosurgical lymphaticovenous anastomosis (LVA).

Materials and Methods: This prospective longitudinal cohort study enrolled 51 women with post-treatment gynecological cancer, including those with unilateral lymphedema (study group, n = 25) and those without (control group, n = 26). Venous blood samples obtained from the study group before and after LVA and those from the controls were sent for next-generation sequencing, which was validated by real-time PCR. Dysregulated gene expression in the study group, relative to expression in the controls, was recorded before LVA. After one month, postoperative changes in the expression of the identified genes were evaluated. Protein-protein interaction (PPI) was used to investigate dysregulated genes whose expression returned to baseline levels after LVA.

Results: Of the 148 preoperative dysregulated genes, which comprised 108 up- and 40 down-regulated genes, 78 genes, consisting of 69 up- and 9 down-regulated genes, showed post-LVA recovery to baseline levels. Through PPI analysis, five functional modules involving immunity, lipid metabolism, oxidative stress, transcriptional regulators, and tumor suppression, as well as six hub genes (*CCL2, LPL, PDK4, FOXO3, EGR1*, and *DUSP5*), were identified. Cross-linking and co-regulated genes between modules were also identified.

Conclusion: Localized lymphedema leads to dysregulated gene expression in circulating monocytes. The current study is the first to identify the hub genes related to lymphedema and demonstrate the recovery of some dysregulated genes after LVA.

Keywords: transcriptome, NGS, real-time PCR, hub gene, functional modules

Introduction

Lymphedema is a chronic, debilitating disease that affects as many as 200 million patients worldwide. In developed countries, cancer is the most frequent secondary cause for lymphedema. The most common risks of cancer-related lymphedema include regional lymphadenectomy, radiotherapy, and chemotherapy.[1] Lower limb lymphedema can occur in up to 70% of selected patients diagnosed with gynecological cancers.[2] This condition has been linked to edema, inflammation, tissue fibrosis, abnormal adipose deposition,[3] and oxidative stress.[4,5] Conservative treatments, such as complex decongestive therapy (CDT), have been shown to decrease inflammatory gene expression after lymphedematous volume reduction.[6] However, due to limitations of CDT, alternative treatment modalities have been considered.

Supermicrosurgical lymphaticovenous anastomosis (LVA) is effective in reducing excess lymphedematous volume by channeling the stagnant lymph into the recipient vein.[7,8] Moreover, post-LVA lymphedematous limb volume reduction is correlated with a decrease in oxidative stress, as we recently demonstrated.[9]

Currently, the systemic impact of cancer-related lower limb lymphedema on gene expression has not been assessed. Some studies have investigated the local dysregulation of gene expression, but these reports specifically focused on adipose-derived mesenchymal stem cells from breast cancer-related lymphedema (BCRL).[10,11] Koc et al demonstrated the effects of lymphedema on miRNA expression in patients with BCRL.[12] Additionally, whether the expression of dysregulated genes is reversible after lymphatic surgical intervention requires further investigation. In the present study, we aimed to profile the expression of dysregulated genes in circulating monocytes of patients with cancer-related lower limb lymphedema, before and after LVA treatment.

Materials and Methods

Study Participants

The institutional review board of Kaohsiung Chang Gung Memorial Hospital (KCGMH) approved this prospective longitudinal cohort study (IRB No.: 201702190B0/201702190B0C501) and this study has complied with the Declaration of Helsinki. Written informed consent was obtained from all patients. The patient cohort was enrolled between November 2019 and September 2021, from KCGMH. The four recruitment criteria were as follows: female patients, 18 years and older, with gynecological cancer; unilateral lower limb lymphedema; lymphedema duration greater than 2 years; and lymphedema confirmed with indocyanine green (ICG) lymphography before surgery. Patients were excluded from the study group based on the following four exclusion criteria: a diagnosis of primary lymphedema, upper limb lymphedema, or bilateral lower limb lymphedema; a history of previous LVA, lymph node transfer, liposuction, or excisional therapy such as the Charles procedure; patients lost to follow-up; or patients with incomplete data. Details of the operative techniques have been previously described.[7] Serum samples from venous blood were collected from the arm before and one month after LVA from the study group. Patients without lymphedema who received treatments for gynecological cancers at the same institution were enrolled as controls with venous serum samples collected for comparison.

Definitions

The severity of the lymphedema was classified based on the International Society of Lymphology (ISL) staging system, namely mild (Stages 0-I) and moderate-to-severe (Stages II–III). Supermicrosurgical LVA was performed by a single senior surgeon with 11–0 nylon sutures (Ethilon, Ethicon, New Jersey, USA) using a high-power surgical microscope (Pentero 900, Carl Zeiss AG, Oberkochen, Germany). The positivity of ICG and flow of a lymphatic vessel (LV) were defined based on microscopic observations. ICG-positive LVs were defined as those that were positive for fluorescence observed at an excitation peak at 789 nm and an emission peak at 814 nm with a microscope-integrated–near-infrared imaging system (Pentero 900, Carl Zeiss AG, Oberkochen, Germany). Microscopically discernible lymphatic flow from the distal opening of a transected LV were defined as flow positive LVs. The diameters of the LVs were determined to a precision of 0.01 mm. The classification of lymphosclerosis was based on intraoperative findings of the four criteria reported in a previous study: wall thickness, appearance, wall expandability, and lumen.[13] All LVs were classified into four categories: s0 (very thin, translucent, expandable with identifiable lumen), s1 (thin, white, expandable with identifiable lumen), s2 (thick, white, not expandable with identifiable lumen), and s3 (very thick, white, not expandable with unidentifiable lumen). For LVs, categories s0 and s1 were considered ideal, s2 suboptimal, and s3 not suitable.

Operative Technique

The first and third interdigital toe webbing and the medial and lateral malleoli were intradermally injected with 0.1 mL of ICG. The linear dermal backflow (DB) pattern of the LV was detected with a handheld near-infrared imaging device (Fluobeam, FluoOptic, Grenoble, France) to guide incision placement. For patients with a diffuse DB pattern where linear patterns could not be observed, incisions were placed along the anatomical location of the great saphenous vein.

The incision was usually 3 cm in length and extended when necessary. LVA was performed using only antegrade LV. The operative techniques were as previously described.[7]

Experimental Design and Sample Preparation

Isolation of Peripheral Blood Mononuclear Cells

Venous blood samples were obtained from the controls and the study group. Peripheral blood mononuclear cells (PBMCs) were separated from whole blood by density gradient centrifugation using Ficoll–Paque Premium (17-5442-02, Merck, Kenilworth, New Jersey, U.S.A.). Specifically, 4 mL of Ficoll solution was added to the bottom of a 15 mL tube before the addition of 8 mL of whole blood. After centrifugation at 400 g for 40 min at 25 °C, PBMCs were collected from the plasma/Ficoll interface.

After PBMC separation, CD14$^+$ cells were isolated using anti-human CD14 magnetic particles (557769, BD Bioscience, Franklin Lakes, New Jersey, U.S.A.). PBMCs were diluted with equal amounts of phosphate-buffered saline and centrifuged at 240 g for 5 min. The supernatant was discarded, and the cell pellets were resuspended in 1X BD IMag™ buffer. Cell numbers were determined, and cell suspensions were centrifuged at 200 g for 10 min. For every 10^7 cells, 50 μL of BD IMag™ anti-human CD14 magnetic particles was added to the supernatant. The cell-magnetic particle mixture was incubated at room temperature for 30 min. After washing with 1X BD IMag™ buffer, pellets of CD14$^+$ cells were collected and resuspended in 500 μL of QIAzol lysis reagent (RLT buffer, RNeasy Mini Kit, Qiagen, Venlo, Netherlands) for further use.

RNA Extraction, Quantification, and Quality Determination

Total RNA was extracted from CD14$^+$ cells using the RNeasy Mini Kit (74104, Qiagen, Venlo, Netherlands) following the manufacturer's instructions. RNA samples were quantified with the NanoDrop 2000 spectrophotometer (Thermo Scientific, Waltham, Massachusetts, USA) and Qubit RNA Assay Kit (Q10210, Thermo Scientific, Waltham, Massachusetts, U.S.A.). RNA quality was assessed using the RNA integrity number (RIN) using a Caliper LabChip Analyzer (PerkinElmer, Waltham, Massachusetts, U.S.A.).

Library Preparation and Sequencing

Libraries were prepared from 1 μg of total RNA using TruSeq Stranded mRNA (15031047, Illumina, San Diego, California, USA) for Illumina® Platforms in accordance with the manufacturer's instructions. Library concentrations were measured using the Qubit dsDNA HS Assay Kit (Q32851, Thermo Fisher, Waltham, Massachusetts, U.S.A.). The quality and concentration of the libraries were determined using an Agilent high sensitivity DNA assay kit (5067-4626, Agilent, Santa Clara, California, U.S.A.). Libraries were sequenced using a NextSeq 500 system (Illumina, San Diego, California, U.S.A.).

Data Analysis

The quality of the FASTQ sequence files was evaluated using FastQC (v0.11.8). STAR (v2.7.3a) was used for RNA-seq read alignment and quantification. The reads were aligned to the human reference genome assembly (hg38). Differential gene expression analysis was performed using DESeq2 (v1.24.0). For genes whose changes in differential expression were over two-fold with an adjusted p-value ≤ 0.05, gene ontology and KEGG pathways were analyzed using goseq (v1.36.0). Genes with restored expression after LVA were imported into the STRING database of known and predicted protein-protein interactions (PPIs) (https://string-db.org).

Real-Time Quantitative Polymerase Chain Reaction (PCR)

From the NGS data, genes exhibiting greater than 2-fold changes in expression were selected for real-time PCR validation. For validation, reverse transcription of CD14 RNA to cDNA was performed using a high-capacity cDNA reverse transcription kit (4368814, Applied Biosystems, Waltham, Massachusetts, USA) according to the manufacturer's instructions. Quantification was conducted using Fast SYBR Green Master Mix (Applied Biosystems, 4385612) and 7500 Real-Time PCR System (Thermo Fisher). Six genes were chosen and the sequences of the primers used were as follows: *GAPDH*, forward 5'-ACAGTCAGCCGCATCTTCTT-3' and reverse 5'-GCCCAATACGACCAAATCC-3';

CCL2, forward 5'-GATCTCAGTGCAGAGGC-3' and reverse 5'-GGTTTGCTTGTCCAGGT-3'; *SLC1A3*, forward 5'-AGCAATGGAGAAGAGCC-3' and reverse 5'-ACAATGACAGCGGTGAC-3'; *SPRY1*, forward 5'-ACCTGCATGTGCTTAGT-3' and reverse 5'-CTTTAGCAGGAGGATAACAGAGTA-3'; *ALOX15B*, forward 5'-TGGAGGAGTCTGAATGAGATG-3' and reverse 5'-GGAAGTTCTTTGGGAGGTAG-3'; *ZBTB16*, forward 5'-CATGGACTTCAGCACCTAT-3' and reverse 5'-ACAGCCTCGTTATCAGGA-3'; *GPI*, forward 5'-CTGCTGGGTATCTGGTACA-3' and reverse 5'-CACACGGGTTCCAGATT-3'. The real-time PCR master mix was prepared as follows: 10 μL 2X Fast SYBR Green Master Mix, 1 μL forward primer (10 μM), 1 μL reverse primer (10 μM), 1 μL cDNA, and 7 μL nuclease-free water. The default PCR thermal cycling conditions were as follows: 20s at 95°C and 40 cycles of 3s at 95°C and 30s at 60°C.

Statistical Analysis

All statistical analyses were performed using GraphPad Prism 6 (GraphPad Software Inc., San Diego, CA, USA). Quantitative interoperative findings are presented as the median with interquartile range (IQR). Real-time PCR data are presented as mean ± standard error. Data analysis of the differences between groups means was performed using one-way analysis of variance, followed by Tukey's honestly significant difference test. Statistical significance was set at $p < 0.05$.

Results

Demographic Data

A total of 51 women with post-treatment gynecological cancer included those with unilateral lymphedema (study group, n=25) and their lymphedema-free counterparts (control group, n=26). When comparing patient characteristics (Table 1), the patients in the study group were found to have a higher incidence of cervical cancer (36.0% vs 0.0%) and

Table 1 Patient Demographics (n=51)

	Study Group Lymphedema	Control Group Lymphedema-Free	*p*-value
Sex, female, n (%)	25 (100)	26 (100)	1.000
Age, years, mean±SD	60.6±8.6	56.8±10.4	0.081
Etiology, cancer type, n (%)			0.002
Cervical	9 (36.0)	0 (0.0)	
Endometrial	11 (44.0)	14 (53.8)	
Ovarian	4 (16.0)	12 (46.2)	
Vulvar	1 (4.0)	0 (0.0)	
ISL Stage (0-I/II–III), n (%)	2(8.0)/23(92.0)	n/a	n/a
BMI, kg/m², mean±SD	25.6±4.9	25.3±4.6	0.840
DM, n (%)	6 (24.0)	5 (19.2)	0.941
HTN, n (%)	7 (28.0)	7 (26.9)	>0.999
Affected limb (Left/Right), n (%)	14 (56.0)/11 (44.0)	n/a	n/a
Chemotherapy, n (%)	9 (36.0)	12 (46.2)	0.651
Radiotherapy, n (%)	11 (44.0)	2 (7.7)	0.008
Duration of post-cancer treatment follow-up, months, median [IQR]	106.0 [42.0, 226.0]	76.5 [66.0, 102.0]	0.423
Duration of LE, year, median [IQR]	1.40 [0.55, 7.24]	n/a	n/a

Notes: Normally distributed data are expressed as mean ± SD (standard deviation); non-normally distributed data are expressed as median [Inter-Quartile Range (IQR), 25–75%].
Abbreviations: ISL, International Lymphology Society; BMI, body mass index; DM, diabetes mellitus; HTN, hypertension; LE, lymphedema; n/a, not applicable.

Table 2 Intraoperative Findings

	Lymphedema Group (n=25)
Total LVA performed	144
LVA performed per patient, median [IQR]	6.0 [4.0, 7.0]
Diameter of LVs, overall, mm, median [IQR]	0.68 [0.51, 0.80]
ICG (+) LVs found, n (%)	109 (75.7)
Diameter, mm, median [IQR]	0.75 [0.57, 0.81]
Lymphosclerosis classification, n, (%)	
s0 (ideal for LVA)	10 (6.9)
s1 (ideal for LVA)	98 (68.1)
s2 (suboptimal for LVA)	29 (20.1)
s3 (not suitable for LVA)	7 (4.9)
Total number of recipient veins	83
Recipient veins per patient median [IQR]	3.0 [2.0, 4.0]
Diameter, mm, median [IQR]	0.97 [0.8, 1.2]

Note: Non-normally distributed data are shown as median (Inter-Quartile Range, 25–75%).
Abbreviations: LVs, lymphatic vessels; LVA, lymphaticovenous anastomosis; ICG (+), indocyanine green-positive.

a significantly ($p = 0.002$) lower occurrence of ovarian cancer (16.0% vs 46.2%) than the patients in the control group. The study group also had a higher prevalence of radiotherapy than the control group (44.0% vs 7.7%, $p = 0.008$). No significant intergroup differences were noted in sex ($p = 1.000$), age ($p = 0.166$), body mass index ($p = 0.840$), diabetes ($p = 0.941$), hypertension ($p > 0.999$), or chemotherapy ($p = 0.651$), and the duration of post-cancer treatment follow-up ($p = 0.423$).

Intraoperative Findings

Supermicrosurgical LVA was performed on the patients of the study group and the intraoperative findings are presented in Table 2. In total, 144 LVs were identified with a median of 6.0 LVAs per patient (IQR 4.0–7.0). The median LV diameter was 0.68 mm (IQR 0.51–0.80 mm). The total number of ICG-positive LVs was 109 (75.7%) with a median diameter of 0.75 mm (IQR 0.57–0.81). Based on the lymphosclerosis classification, 10 s0 (6.9%), 98 s1 (68.1%), 29 s2 (20.1%), and 7 s3 (4.9%) LVs were identified. A total of 83 recipient veins were identified with a median of 3.0 (IQR 2.0–4.0) recipient veins per patient and a median diameter of 0.97 mm (IQR 0.8–1.2).

Gene Expression Analysis

Next-generation sequencing (NGS) was used to evaluate gene expression before and one month after LVA. Expression analysis was conducted to compare the study and control groups, with 10 patients from each group, to identify genes that were dysregulated prior to LVA and those that were restored to baseline levels following LVA. Before LVA, a total of 148 dysregulated genes were identified by NGS, which included 108 up- and 40 down-regulated genes, compared to the controls. After LVA, 78 out of the 148 previously dysregulated genes restored to baseline expression, including 69 upregulated genes (63 protein-coding, six non-coding) and nine genes with down-regulated expression (Figure 1). Six of these genes exhibited greatest fold changes in expression were selected, namely *GPI, SPYR1, SLC1A3, ZBTB16, ALOX15B*, and *CCL2* for real-time PCR validation of NGS data. These genes exhibited fold changes in expression ranging from 2.3 to 8.8. Venous blood samples from the study group (15
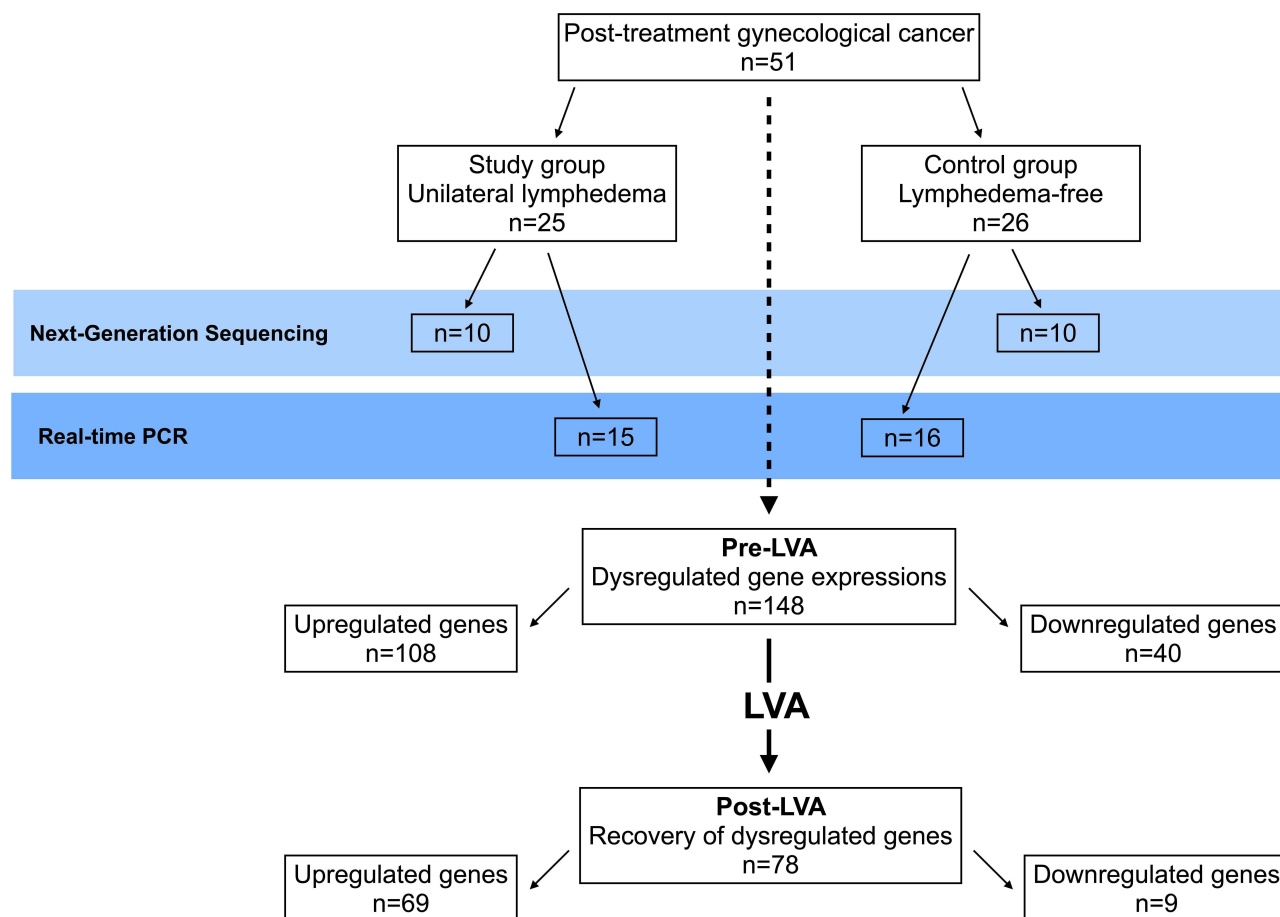
Figure 1 Summary. Fifty-one women with post-treatment gynecological cancer, including those with unilateral lymphedema (study group, n=25) and those without (control group, n=26). Venous blood samples obtained from the study group before and after LVA and those from the controls were sent for next-generation sequencing, which was validated by real-time PCR. Before LVA, 148 dysregulated genes were identified by NGS. Compared to the controls, 108 and 40 up- and downregulated genes were detected, respectively. After LVA, expression of 78 of the genes was restored to near baseline levels. Of these, 69 had been upregulated (63 protein coding genes, six non-coding genes) and nine had been downregulated.

patients) and the controls (16 patients) were used for the validation. Of the six selected genes, four with significantly upregulated expression prior to LVA (*SPYR1, SLC1A3, ZBTB16,* and *ALOX15B*) were found to return to baseline levels following LVA, however *GPI* remained upregulated after LVA. *CCL2* was downregulated before LVA, but did not change significantly following LVA, although there was a slight increase. These findings are compatible with the expression patterns observed using NGS (Figure 2). In compliance with Reviewer's opinion regarding the correlations between the changes in gene expression and limb volume before and after LVA, the percentage reduction of post-LVA limb volume were calculated from nine out of 15 patients in the study group who have completed their pre- and 6 months post-LVA MR volumetry. These data were compared with six genes selected for real-time PCR validation of NGS data (Figure 2). These results were shown in Supplemental Figures 1 and 2, demonstrating correlations between the changes in gene expressions and limb volume reduction. The results of Gene Ontology were shown in Supplemental Figures 3 and 4, and KEGG analysis were shown as Supplemental Table 1 and Supplemental Figures 5–8.

Protein–Protein Interaction and Hub Genes

A schematic representation of the PPI network consisting of 28 interconnecting genes is presented in Figure 3. The approach revealed five functional modules involving immunity, lipid metabolism, oxidative stress, transcriptional regulators, and tumor suppression (Table 3). Six hub genes, namely genes carrying the highest degree of connectivity, were also identified. Module 1 (immunity), contained eight genes: C-C motif chemokine ligand 2 (*CCL2*, hub gene);
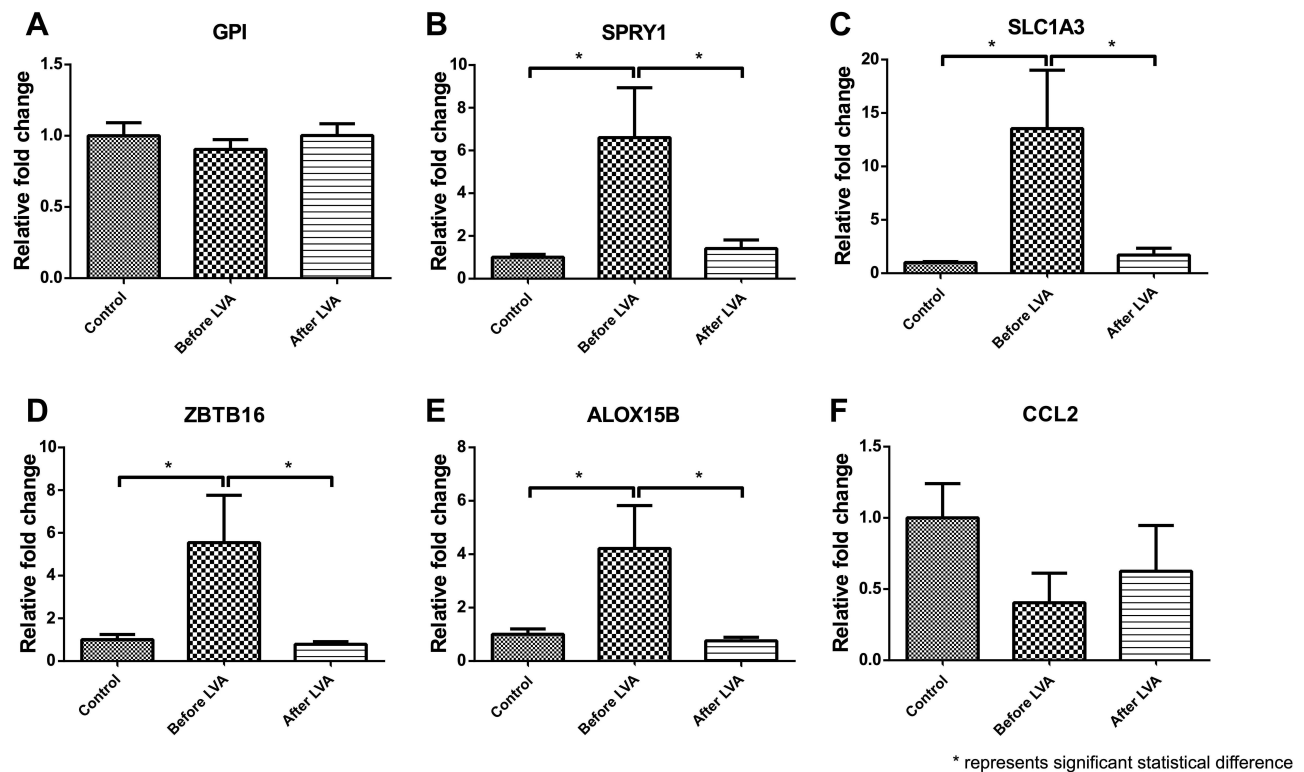
Figure 2 Next-Generation Sequencing (NGS) validation with real-time PCR. From the 72 genes that demonstrated recovery to baseline levels after LVA, gene expressions with fold changes greater than two were selected for NGS validation with real-time PCR. *GPI, SPRY1, SLC1A3, ZBTB16, ALOX15B,* and *CCL2* with gene expression ranging from 2.3- to 8.8-fold changes were selected and analyzed by real-time PCR. The results were (**A**) *GPI* was an upregulated gene before LVA and remained upregulated after LVA; (**B–E**) *SPYR1, SLC1A3, ZBTB16,* and *ALOX15B* showed significantly upregulated expressions before LVA and were restored to baseline expression after LVA; (**F**) *CCL2* was down-regulated before LVA but demonstrated no significant post-LVA change. These findings validated the NGS data. *In the figure represented statistical significant difference.

scavenger receptor cysteine-rich type 1 protein M130 (*CD163*); adenosine receptor A3 (*ADORA3*); P2Y puriceptor 1 (*P2RY1*); C-type lectin domain family 4 member E (*CLEC4E*); interleukin 1 receptor type 2 (*IL1R2*); interleukin 1 receptor accessory protein (*IL1RAP*); and enoyl-CoA hydratase domain containing 3 (*ECHDC3*). Module 2 (lipid metabolism) comprised four genes: lipoprotein lipase (*LPL*, hub gene); pyruvate dehydrogenase kinase 4 (*PDK4*, hub gene); long-chain-fatty-acid-CoA ligase 1 (*ACSL1*); and perilipin-2 (*PLIN2*). Module 3 (oxidative stress), contained three genes: forkhead box O3 (*FOXO3*, hub gene); sestrin-1 (*SESN1*); and protein SCO2 homolog, mitochondrial (*SCO2*). Module 4 (transcriptional regulators), comprised seven genes: early growth response protein 1 (*EGR1*, hub gene); immediate early response gene 2 protein (*IER2*); protein BTG2 (*BTG2*); nuclear receptor subfamily 4 group A member 1 (*NR4A1*); cyclin-dependent kinase 5 activator 1 (*CDK5R1*); protein C-ets-2 (*ETS2*); Kruppel-like factor 7 (*KLF7*); nuclear factor I A-type (*NFIA*); solute carrier family 1 member 3 gene (*SLC1A3*); and polyhomeotic-like protein 2 (*PHC2*). Module 5 (tumor suppression), contained three genes: dual specificity phosphatase 5 (*DUSP5*, hub gene); mitogen-activated protein kinase kinase kinase 8 (*MAP3K8*); and protein sprouty homolog 1 (*SPYR1*). Downregulated hub genes comprised *CCL2, EGR1*, and *DUSP5*, while upregulated hub genes consisted of *LPL, PDK4*, and *FOXO3*.

Discussion

The current study is the first to identify the hub genes related to lymphedema and demonstrate the recovery of some dysregulated genes after LVA. In contrast to most previous studies that investigated the changes in gene expression in lymphedematous adipose tissue, we focused on the systemic effects of lower limb lymphedema on circulating monocytes. Of the 148 genes with dysregulated expression in circulating monocytes, 78 (69 upregulated and nine down-regulated) showed restoration of expression levels after LVA. For 28 of these genes, we were able to classify them using
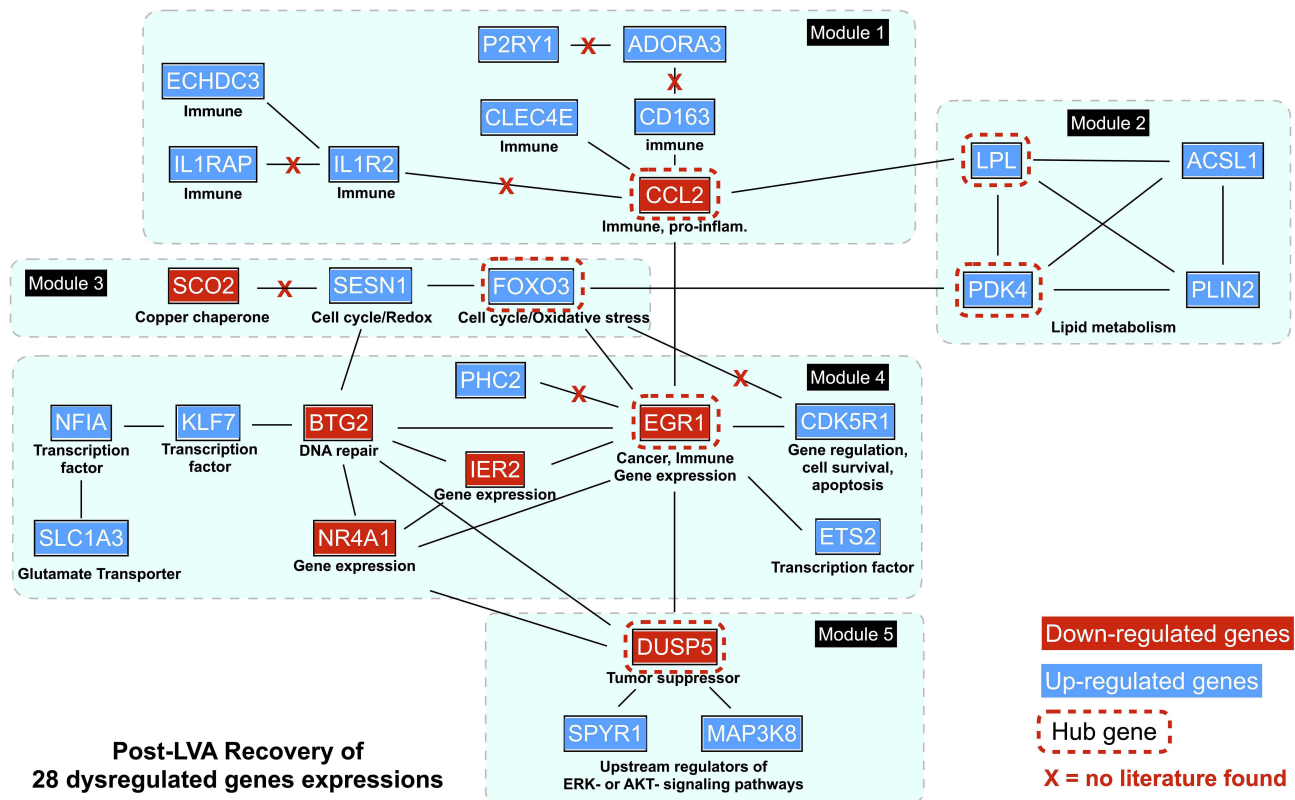
Figure 3 The protein-protein interaction (PPI), functional modules, and hub genes. Five functional modules and six hub genes were identified from the PPI networks that comprised 28 interconnecting genes. Module 1, which is involved with immunity, contained the hub gene, CCL2; Module 2, which is associated with lipid metabolism, included the hub genes LPL and PDK4; Module 3, which is linked to oxidative stress, contained the hub gene FOXO3; Module 4, which is associated with transcriptional regulators, contained the hub gene EGR1; Module 5, which is related to tumor suppression, contained the hub gene DUSP5. Downregulated genes are colored in red; upregulated genes are colored in blue.

PPI interconnections into five functional modules with six hub genes. A particularly interesting observation is that the six identified hub genes are reportedly associated with oxidative stress.[14–26] This finding is in accordance with our recent study regarding the alleviation of oxidative stress in lower limb lymphedema following LVA.[9]

The discovery of functional modules and hub genes may shed light on the mechanisms underlying lymphedema. In Module 1, which consisted of immune-related genes, the hub gene *CCL2* is a pro-inflammatory chemokine that recruits monocytes[14] and is associated with the development of breast cancer[15–17] and colorectal cancer.[18] Oxidative stress is known to increase *CCL2* mRNA level.[19,20] The ablation or blockade of the *CCL2* gene has been reported to reduce oxidative stress and increase the expression of anti-inflammatory macrophage markers.[21,22] Although upregulation of *CCL2* was expected during lymphedema in the presence of elevated oxidative stress, it was instead found to be downregulated in the local lower limb adipose tissues of patients with lymphedema.[11] Our observation of downregulated *CLL2* expression in circulating monocytes may suggest a different oxidative stress regulatory mechanism in the context of secondary lymphedema that deserves further investigation.

Module 2 appears to be involved in lipid metabolism and was composed of abnormally upregulated genes controlling the adipocytokine signaling pathways involving the hub genes *LPL* and *PDK4*. Both genes were upregulated, but baseline expression was restored after LVA. A previous study demonstrated that tissue swelling in BCRL, which is attributed to both fluid accumulation and fat deposition,[23] is associated with a significantly higher expression of LPL,[10] which is known to be involved in lipid uptake, lipolysis, and fatty acid utilization.[24–26] Several studies have suggested that oxidative stress is positively correlated with LPL production in macrophages.[27–30] In addition, exercise-induced oxidative stress has been found to increase *PDK4* gene expression.[31] Consistent with this, a previous RNA sequencing study showed a strong association between positive *LPL* and *PDK4* expression and oxidative stress.[32] Moreover, our

Table 3 Functional Modules and Hub Genes Identified from 28 Interconnected Genes

Module 1 (8 Genes)	
*CCL2	C-C motif chemokine ligand 2
CD163	Cluster of Differentiation 163
ADORA3	Adenosine A3 Receptor
P2RY1	Purinergic Receptor P2Y1
CLEC4E	C-Type Lectin Domain Family 4 Member E
IL1R2	Interleukin 1 Receptor Type 2
IL1RAP	Interleukin 1 Receptor Accessory Protein
ECHDC3	Enoyl-CoA Hydratase Domain Containing 3
Module 2 (4 Genes)	
*LPL	Lipoprotein lipase
*PDK4	Pyruvate dehydrogenase kinase 4
ACSL1	Acyl-CoA Synthetase Long Chain Family Member 1
PLIN2	Perilipin 2
Module 3 (3 Genes)	
*FOXO3	Forkhead box O3
SESN1	Sestrin 1
SCO2	Supercritical Carbon Dioxide
Module 4 (7 Genes)	
*EGR1	Early Growth Response 1
IER2	Immediate Early Response 2
BTG2	B-cell translocation gene 2
NR4A1	Nuclear Receptor Subfamily 4 Group A Member 1
CDK5R1	Cyclin Dependent Kinase 5 Regulatory Subunit 1
ETS2	ETS Proto-Oncogene 2, Transcription Factor
PHC2	Polyhomeotic Homolog 2
KLF7	Krueppel-like factor 7
NFIA	Nuclear factor 1 A-type
SLC1A3	Excitatory amino acid transporter 1
Module 5 (3 Genes)	
*DUSP5	Dual Specificity Phosphatase 5
MAP3K8	Mitogen-Activated Protein Kinase Kinase Kinase 8
SPYR1	Mycobacterium sp. Spyr1

Note: *Hub gene.

recent study demonstrated that elevated oxidative stress in lower limb lymphedema can be reduced by LVA.[9] The decline in oxidative stress after LVA may, therefore, have contributed to the observed restoration of LPL and PDK4 expression.

Module 3 contained *FOXO3* as a hub gene, which is a hypoxic stress-responsive transcription factor known to protect against oxidative stress in the kidney[33–35] and the heart.[36,37] Oxidative stress has been shown to induce *FOXO3* and peroxiredoxin 2 (*PRDX2*) gene expression.[38] PRDX2 is a thioredoxin-dependent peroxidase that functions as a defense system against reactive oxygen species.[39] In the present study, the abnormally upregulated preoperative *FOXO3* expression was restored after LVA. Furthermore, our previous study demonstrated an association between a reduction in *PRDX2* expression and a decrease in oxidative stress after LVA.[9] Therefore, the co-expression of *FOXO3* and *PRDX2* may be related to the level of oxidative stress in lower limb lymphedema.

Module 4 contained the key hub gene, *EGR1*, which not only plays a vital role in regulating cell differentiation, growth, and survival, but is also a mediator of inflammatory gene expression and tumor cell metastasis.[40–42] Oxidative stress downregulates *EGR1* expression in cardiomyocytes,[43] which is consistent with the findings of our study. Module 5

was composed of genes coding for upstream regulators of the ERK or AKT signaling pathway, including DUSP5.[44–46] It is involved in T-cell activation,[47] anti-inflammation,[48] and acts as a negative regulator of the mitogen-activated protein kinase pathway.[49,50] DUSP5 also serves as a tumor suppressor in human cancers.[51–53] Consistently, its downregulation is associated with increased cardiac oxidative stress[45] and observed in cervical, ovarian, and breast cancers.[49,54,55]

Interestingly, a few sets of co-regulated genes were found within different modules in the present investigation, as well as in other studies. For example, co-regulated *LPL, PLIN2*, and *ACSL1* gene expression in Module 2 is also related to lipolysis and fatty acid utilization.[25] *FOXO3* and *SESN1* in Module 3 also work synergistically to regulate the responses to oxidative stress.[56] Moreover, cross-linking among different modules by gene co-regulation was observed in the present study. Furthermore, concomitant *CCL2* (Module 1) downregulation and *LPL* (Module 2) upregulation has been shown to be associated with an increased body mass index.[57]

The limitations of this study include the lack of normal healthy controls to show the difference between patients with lymphedema and those with good health. The extent of oxidative stress was not measured in the present study due to the limited sample availability. Although six genes were analyzed by real-time PCR, the validation of all dysregulated genes would provide more comprehensive evidence. In summary, although the reduction in post-LVA oxidative stress may be linked to the post-LVA recovery of dysregulated genes, more evidence is required to validate this hypothesis. Whether there is a causal correlation between oxidative stress and lymphedema requires further investigation.

Conclusion

Localized lymphedema leads to dysregulated gene expression in circulating monocytes. The current study identified hub genes related to lymphedema and demonstrated the restoration of some dysregulated genes after LVA. A thorough under-standing of the pathophysiological changes that may result in lymphedema requires further investigation. The present study may provide some basic information that can help in the advancement of lymphedema research at the molecular level.

Abbreviations

ACSL1, Acyl-CoA Synthetase Long Chain Family Member 1; ADORA3, Adenosine A3 Receptor; BCRL, breast cancer-related lymphedema; BTG2, B-cell translocation gene 2; CCL2, C-C Motif Chemokine Ligand 2; CD163, Cluster of Differentiation 163; CDK5R1, Cyclin Dependent Kinase 5 Regulatory Subunit 1; CLEC4E, C-Type Lectin Domain Family 4 Member E; DB, dermal backflow; DUSP5, Dual Specificity Phosphatase 5; ECHDC3, Enoyl-CoA Hydratase Domain Containing 3; EGR1, Early Growth Response 1; ETS2, ETS Proto-Oncogene 2 Transcription Factor; FOXO3, Forkhead box O3; ICG, indocyanine green; IER2, Immediate Early Response 2; IL1R2, Interleukin 1 Receptor Type 2; IL1RAP, Interleukin 1 Receptor Accessory Protein; IQR, interquartile range; ISL, International Society of Lymphology; LPL, Lipoprotein lipase; LV, lymphatic vessel; LVA, lymphaticovenous anastomosis; MAP3K8, Mitogen-Activated Protein Kinase Kinase Kinase 8; NGS, next-generation sequencing; NR4A1, Nuclear Receptor Subfamily 4 Group A Member 1; P2RY1, Purinergic Receptor P2Y1; PBMC, peripheral blood mononuclear cell; PBS, phosphate-buffered saline; PDK4, Pyruvate Dehydrogenase Kinase 4; PHC2, Polyhomeotic Homolog 2; PLIN2, Perilipin 2; PPI, protein-protein interaction; RIN, RNA integrity number; SCO2, Supercritical Carbon Dioxide; SESN1, Sestrin 1; SPYR1, Mycobacterium sp Spyr1.

Data Sharing Statement

Data is available upon request.

Ethics Approval and Informed Consent

This study was approved by the Institutional Review Board of Chang Gung Memorial Hospital (Approval number: 201702190B0/201702190B0C501).

Consent for Publication

The images and tables can be published, and that the person(s) providing consent have been shown the article contents to be published.

Acknowledgments

Author Contributions

All authors made a significant contribution to the work reported, whether that is in the conception, study design, execution, acquisition of data, analysis and interpretation, or in all these areas; took part in drafting, revising or critically reviewing the article; gave final approval of the version to be published; have agreed on the journal to which the article has been submitted; and agree to be accountable for all aspects of the work.

Funding

Disclosure

None of the authors has a financial interest in any of the products, devices, or drugs mentioned in this manuscript.

References

1. Grada AA, Phillips TJ. Lymphedema: pathophysiology and clinical manifestations. *J Am Acad Dermatol*. 2017;77(6):1009–1020. doi:10.1016/j.jaad.2017.03.022
2. Dessources K, Aviki E, Leitao MM Jr. Lower extremity lymphedema in patients with gynecologic malignancies. *Int J Gynecol Cancer*. 2020;30(2):252–260. doi:10.1136/ijgc-2019-001032
3. Sung CJ, Wang SX, Hsu JF, Yu RP, Wong AK. Current understanding of pathological mechanisms of lymphedema. *Adv Wound Care*. 2021. doi:10.1089/wound.2021.0041
4. Beier A, Siems W, Brenke R, Grune T. [Increased formation of free radicals in chronic lymphedema]. *Z Lymphol*. 1994;18(1):8–11. German.
5. Siems WG, Brenke R, Beier A, Grune T. Oxidative stress in chronic lymphoedema. *QJM*. 2002;95(12):803–809. doi:10.1093/qjmed/95.12.803
6. Foldi E, Sauerwald A, Hennig B. Effect of complex decongestive physiotherapy on gene expression for the inflammatory response in peripheral lymphedema. *Lymphology*. 2000;33(1):19–23.
7. Yang JC, Wu SC, Chiang MH, Lin WC, Chiang PL, Hsieh CH. Supermicrosurgical lymphaticovenous anastomosis as an alternative treatment option for moderate-to-severe lower limb lymphedema. *J Am Coll Surg*. 2020;230(2):216–227. doi:10.1016/j.jamcollsurg.2019.10.007
8. Yang JC, Yen YH, Wu SC, Lin WC, Chiang MH, Hsieh CH. Supermicrosurgical lymphaticovenous anastomosis as an alternative treatment option for patients with lymphorrhea. *Plast Reconstr Surg*. 2019;144(5):1214–1224. doi:10.1097/PRS.0000000000006169
9. Yang JC, Huang LH, Wu SC, et al. Lymphaticovenous anastomosis supermicrosurgery decreases oxidative stress and increases antioxidant capacity in the serum of lymphedema patients. *J Clin Med*. 2021;10(7):1540. doi:10.3390/jcm10071540
10. Levi B, Glotzbach JP, Sorkin M, et al. Molecular analysis and differentiation capacity of adipose-derived stem cells from lymphedema tissue. *Plast Reconstr Surg*. 2013;132(3):580–589. doi:10.1097/PRS.0b013e31829ace13
11. Xiang Q, Xu F, Li Y, et al. Transcriptome analysis and functional identification of adipose-derived mesenchymal stem cells in secondary lymphedema. *Gland Surg*. 2020;9(2):558–574. doi:10.21037/gs.2020.02.09
12. Koc M, Wald M, Varaliova Z, et al. Lymphedema alters lipolytic, lipogenic, immune and angiogenic properties of adipose tissue: a hypothesis-generating study in breast cancer survivors. *Sci Rep*. 2021;11(1):8171. doi:10.1038/s41598-021-87494-3
13. Yamamoto T, Yamamoto N, Yoshimatsu H, Narushima M, Koshima I. Factors associated with lymphosclerosis: an analysis on 962 lymphatic vessels. *Plast Reconstr Surg*. 2017;140(4):734–741. doi:10.1097/PRS.0000000000003690
14. Zollbrecht C, Grassl M, Fenk S, et al. Expression pattern in human macrophages dependent on 9p21.3 coronary artery disease risk locus. *Atherosclerosis*. 2013;227(2):244–249. doi:10.1016/j.atherosclerosis.2012.12.030
15. Qian BZ, Li J, Zhang H, et al. CCL2 recruits inflammatory monocytes to facilitate breast-tumour metastasis. *Nature*. 2011;475(7355):222–225. doi:10.1038/nature10138
16. Li D, Ji H, Niu X, et al. Tumor-associated macrophages secrete CC-chemokine ligand 2 and induce tamoxifen resistance by activating PI3K/Akt/mTOR in breast cancer. *Cancer Sci*. 2020;111(1):47–58. doi:10.1111/cas.14230
17. Szekely B, Bossuyt V, Li X, et al. Immunological differences between primary and metastatic breast cancer. *Ann Oncol*. 2018;29(11):2232–2239. doi:10.1093/annonc/mdy399
18. De la Fuente Lopez M, Landskron G, Parada D, et al. The relationship between chemokines CCL2, CCL3, and CCL4 with the tumor microenvironment and tumor-associated macrophage markers in colorectal cancer. *Tumour Biol*. 2018;40(11):1010428318810059. doi:10.1177/1010428318810059
19. Uchiyama T, Itaya-Hironaka A, Yamauchi A, et al. Intermittent hypoxia up-regulates CCL2, RETN, and TNFalpha mRNAs in adipocytes via down-regulation of miR-452. *Int J Mol Sci*. 2019;20(8):1960. doi:10.3390/ijms20081960
20. Kumar A, Shalmanova L, Hammad A, Christmas SE. Induction of IL-8(CXCL8) and MCP-1(CCL2) with oxidative stress and its inhibition with N-acetyl cysteine (NAC) in cell culture model using HK-2 cell. *Transpl Immunol*. 2016;35:40–46. doi:10.1016/j.trim.2016.02.003

21. Luciano-Mateo F, Cabre N, Fernandez-Arroyo S, et al. Chemokine (C-C motif) ligand 2 gene ablation protects low-density lipoprotein and paraoxonase-1 double deficient mice from liver injury, oxidative stress and inflammation. *Biochim Biophys Acta Mol Basis Dis*. 2019;1865 (6):1555–1566. doi:10.1016/j.bbadis.2019.03.006

22. Seok SJ, Lee ES, Kim GT, et al. Blockade of CCL2/CCR2 signalling ameliorates diabetic nephropathy in db/db mice. *Nephrol Dial Transplant*. 2013;28(7):1700–1710. doi:10.1093/ndt/gfs555

23. Brorson H, Svensson H. Complete reduction of lymphoedema of the arm by liposuction after breast cancer. *Scand J Plast Reconstr Surg Hand Surg*. 1997;31(2):137–143. doi:10.3109/02844319709085480

24. Mulumba M, Jossart C, Granata R, et al. GPR103b functions in the peripheral regulation of adipogenesis. *Mol Endocrinol*. 2010;24(8):1615–1625. doi:10.1210/me.2010-0010

25. Bi Y, Yuan X, Chen Y, Chang G, Chen G. Expression analysis of genes related to lipid metabolism in peripheral blood lymphocytes of chickens challenged with reticuloendotheliosis virus. *Poult Sci*. 2021;100(5):101081. doi:10.1016/j.psj.2021.101081

26. Rogers C, Moukdar F, McGee MA, et al. EGF receptor (ERBB1) abundance in adipose tissue is reduced in insulin-resistant and type 2 diabetic women. *J Clin Endocrinol Metab*. 2012;97(3):E329–E340. doi:10.1210/jc.2011-1033

27. Renier G, Desfaits AC, Lambert A, Mikhail R. Role of oxidant injury on macrophage lipoprotein lipase (LPL) production and sensitivity to LPL. *J Lipid Res*. 1996;37(4):799–809. doi:10.1016/S0022-2275(20)37578-7

28. Maingrette F, Renier G. Leptin increases lipoprotein lipase secretion by macrophages: involvement of oxidative stress and protein kinase C. *Diabetes*. 2003;52(8):2121–2128. doi:10.2337/diabetes.52.8.2121

29. Peng J, Lv YC, He PP, et al. Betulinic acid downregulates expression of oxidative stress-induced lipoprotein lipase via the PKC/ERK/c-Fos pathway in RAW264.7 macrophages. *Biochimie*. 2015;119:192–203. doi:10.1016/j.biochi.2015.10.020

30. Oliveira JVB, Lima RPA, Pordeus Luna RC, et al. The direct correlation between oxidative stress and LDL-C levels in adults is maintained by the Friedewald and Martin equations, but the methylation levels in the MTHFR and ADRB3 genes differ. *PLoS One*. 2020;15(12):e0239989. doi:10.1371/journal.pone.0239989

31. Townsend LK, Weber AJ, Barbeau PA, Holloway GP, Wright DC. Reactive oxygen species-dependent regulation of pyruvate dehydrogenase kinase-4 in white adipose tissue. *Am J Physiol Cell Physiol*. 2020;318(1):C137–C149. doi:10.1152/ajpcell.00313.2019

32. Andersen E, Ingerslev LR, Fabre O, et al. Preadipocytes from obese humans with type 2 diabetes are epigenetically reprogrammed at genes controlling adipose tissue function. *Int J Obes*. 2019;43(2):306–318. doi:10.1038/s41366-018-0031-3

33. Li L, Kang H, Zhang Q, D'Agati VD, Al-Awqati Q, Lin F. FoxO3 activation in hypoxic tubules prevents chronic kidney disease. *J Clin Invest*. 2019;129(6):2374–2389. doi:10.1172/JCI122256

34. Deng A, Ma L, Zhou X, Wang X, Wang S, Chen X. FoxO3 transcription factor promotes autophagy after oxidative stress injury in HT22 cells. *Can J Physiol Pharmacol*. 2021;99(6):627–634. doi:10.1139/cjpp-2020-0448

35. Nlandu-Khodo S, Osaki Y, Scarfe L, et al. Tubular beta-catenin and FoxO3 interactions protect in chronic kidney disease. *JCI Insight*. 2020;5(10). doi:10.1172/jci.insight.135454

36. Wang LF, Huang CC, Xiao YF, et al. CD38 deficiency protects heart from high fat diet-induced oxidative stress via activating Sirt3/FOXO3 pathway. *Cell Physiol Biochem*. 2018;48(6):2350–2363. doi:10.1159/000492651

37. Lv W, Jiang J, Li Y, Fu L, Meng F, Li J. MiR-302a-3p aggravates myocardial ischemia-reperfusion injury by suppressing mitophagy via targeting FOXO3. *Exp Mol Pathol*. 2020;117:104522. doi:10.1016/j.yexmp.2020.104522

38. Miyamoto N, Izumi H, Miyamoto R, et al. Nipradilol and timolol induce Foxo3a and peroxiredoxin 2 expression and protect trabecular meshwork cells from oxidative stress. *Invest Ophthalmol Vis Sci*. 2009;50(6):2777–2784. doi:10.1167/iovs.08-3061

39. Lee YJ. Knockout mouse models for peroxiredoxins. *Antioxidants*. 2020;9(2):182.

40. Banerji R, Saroj SD. Early growth response 1 (EGR1) activation in initial stages of host-pathogen interactions. *Mol Biol Rep*. 2021;48 (3):2935–2943. doi:10.1007/s11033-021-06305-0

41. Wang B, Guo H, Yu H, Chen Y, Xu H, Zhao G. The role of the transcription factor EGR1 in cancer. *Front Oncol*. 2021;11:642547. doi:10.3389/fonc.2021.642547

42. Li TT, Liu MR, Pei DS. Friend or foe, the role of EGR-1 in cancer. *Med Oncol*. 2019;37(1):7. doi:10.1007/s12032-019-1333-6

43. Li J, Gong L, Zhang R, et al. Fibroblast growth factor 21 inhibited inflammation and fibrosis after myocardial infarction via EGR1. *Eur J Pharmacol*. 2021;910:174470. doi:10.1016/j.ejphar.2021.174470

44. Gruosso T, Garnier C, Abelanet S, et al. MAP3K8/TPL-2/COT is a potential predictive marker for MEK inhibitor treatment in high-grade serous ovarian carcinomas. *Nat Commun*. 2015;6:8583. doi:10.1038/ncomms9583

45. Xu Z, Tong Q, Zhang Z, et al. Inhibition of HDAC3 prevents diabetic cardiomyopathy in OVE26 mice via epigenetic regulation of DUSP5-ERK1/2 pathway. *Clin Sci*. 2017;131(15):1841–1857. doi:10.1042/CS20170064

46. Ng KY, Chan LH, Chai S, et al. TP53INP1 downregulation activates a p73-dependent dusp10/erk signaling pathway to promote metastasis of hepatocellular carcinoma. *Cancer Res*. 2017;77(17):4602–4612. doi:10.1158/0008-5472.CAN-16-3456

47. Chuang HC, Tan TH. MAP4K family kinases and DUSP family phosphatases in T-cell signaling and systemic lupus erythematosus. *Cells*. 2019;8 (11):1433. doi:10.3390/cells8111433

48. Seo H, Cho YC, Ju A, et al. Dual-specificity phosphatase 5 acts as an anti-inflammatory regulator by inhibiting the ERK and NF-kappaB signaling pathways. *Sci Rep*. 2017;7(1):17348. doi:10.1038/s41598-017-17591-9

49. Liu T, Sun H, Liu S, et al. The suppression of DUSP5 expression correlates with paclitaxel resistance and poor prognosis in basal-like breast cancer. *Int J Med Sci*. 2018;15(7):738–747. doi:10.7150/ijms.24981

50. Chen HF, Chuang HC, Tan TH. Regulation of dual-specificity phosphatase (DUSP) ubiquitination and protein stability. *Int J Mol Sci*. 2019;20 (11):2668.

51. Png CW, Weerasooriya M, Guo J, et al. DUSP10 regulates intestinal epithelial cell growth and colorectal tumorigenesis. *Oncogene*. 2016;35 (2):206–217. doi:10.1038/onc.2015.74

52. Ding J, Li J, Wang H, et al. Long noncoding RNA CRNDE promotes colorectal cancer cell proliferation via epigenetically silencing DUSP5/CDKN1A expression. *Cell Death Dis*. 2017;8(8):e2997. doi:10.1038/cddis.2017.328

53. Kidger AM, Rushworth LK, Stellzig J, et al. Dual-specificity phosphatase 5 controls the localized inhibition, propagation, and transforming potential of ERK signaling. *Proc Natl Acad Sci U S A*. 2017;114(3):E317–E326. doi:10.1073/pnas.1614684114

54. Min H, He W. Long non-coding RNA ARAP1-AS1 promotes the proliferation and migration in cervical cancer through epigenetic regulation of DUSP5. *Cancer Biol Ther.* 2020;21(10):907–914. doi:10.1080/15384047.2020.1806641

55. Wang L, Hu J, Qiu D, et al. Dual-specificity phosphatase 5 suppresses ovarian cancer progression by inhibiting IL-33 signaling. *Am J Transl Res.* 2019;11(2):844–854.

56. Donlon TA, Morris BJ, Chen R, et al. FOXO3 longevity interactome on chromosome 6. *Aging Cell.* 2017;16(5):1016–1025. doi:10.1111/acel.12625

57. Canzoneri R, Naipauer J, Stedile M, et al. Identification of an AP1-ZFP36 regulatory network associated with breast cancer prognosis. *J Mammary Gland Biol Neoplasia.* 2020;25(2):163–172. doi:10.1007/s10911-020-09448-1